

# DESIGN, SYNTHESIS, AND FUNCTIONAL CHARACTERIZATION OF BIODEGRADABLE POLYMERIC NANOPARTICLES FOR TARGETED DRUG DELIVERY APPLICATION

**Khem Lal**

Research Scholar (Chemistry) ISBM University Gariyaband Chhattisgarh

**Dr. Sushrita Patnayak (Assistant Professor)**

Research Supervisor, School of Science, ISBM University Gariyaband Chhattisgarh

---

## ABSTRACT

*Developing targeted medication delivery systems seems to be an excellent strategy for enhancing therapeutic efficacy while decreasing adverse effects. This project primarily aims to develop, create, and test biodegradable polymeric nanoparticles for targeted medication delivery. The selection of biodegradable polymers was based on their compatibility with living organisms, their ability to decompose without harm, and their ability to release any medications contained inside them in a biological environment without risk. Popular techniques such as emulsification, liquid evaporation, and nanoprecipitation were used to create the nanoparticles. This guaranteed that the particles met the requirements for size, stability, and drug encapsulation efficacy. The physical features of the synthesized nanoparticles, including their size, shape, surface charge, drug loading capacity, and drug release rates, were meticulously investigated using state-of-the-art analytical techniques. Additionally, particular ligands were added to the surface of the nanoparticles by functionalization procedures, enabling personalized transport. Their ability to locate and adhere to specific cells or tissues was enhanced as a result. The behavior of drug release, cellular absorption, and damage were examined by in vitro studies. Findings demonstrated that pharmacological delivery to cells was improved, and that release patterns were controllable. Conclusions Biodegradable polymeric nanoparticles provide a versatile and practical method for targeted medication delivery.*

**Keywords:** Design, Synthesis, Nanoparticles, Drug, Application

## INTRODUCTION

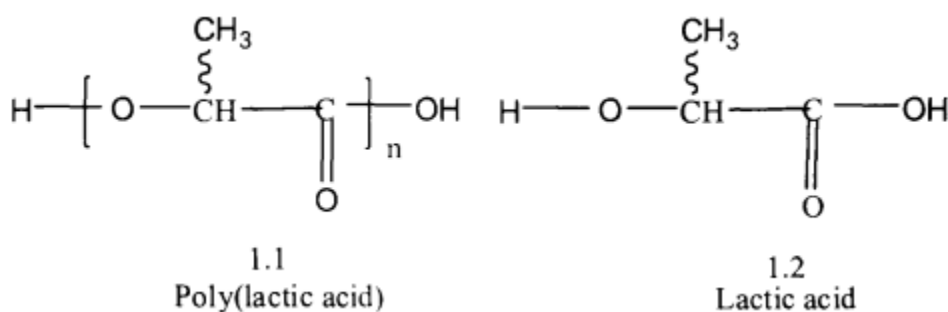
Since the 1940s, polymers made from synthetic petrochemicals have greatly impacted the manufacturing industry. Two major drawbacks remain unaddressed despite the many advantages offered by these materials. The production of these materials requires nonrenewable resources, and these large-scale commodity polymers eventually end up somewhere. There has long been speculation that biodegradable polymers would replace eco-friendly polymers due to their distinctive properties. Numerous useful uses, from simple packaging to advanced biological devices, have emerged as a consequence of the tremendous progress achieved in the synthesis, production, and processing of these materials during the last 30 years. Linear aliphatic polyesters, especially those made from lactic acid (LA), are the most used and well-liked of the several varieties of biodegradable polymers now on the market. Biodegradability and compostability are being defined and tested in a variety of settings by a number of major international organizations. Among these groups are the following: the Organic Reclamation and Composting Association (ORCA), the International Standardization Organization (ISO), the Institute for Standards Research (ISR), the European Standardization Committee (CEN), the German Institute for Standardization (DIN), the Italian Standardization Agency (UNI), and the American Society for Testing and Materials (ASTM). A material's biodegradability is defined according to a specific disposal environment and a specific standard test procedure in each of the current standards (ASTM, CEN, and ISO). This is so even if there isn't currently a universally accepted definition of biodegradable polymers.

An additional quality that needs to be thought about when dealing with thermoplastics is their biodegradability. Thermoplastics are defined by their ability to remain stable while usage but to break down and eventually become part of the natural biological cycle after enough time has elapsed.

Aliphatic ester linkages, the building blocks of poly (lactic acid) (PLA, 1.1), are hydrolysable by enzymes and

chemicals. Proteases, proteinases K, bromelain, esterase, and trypsin are among the many enzymes that hydrolyze PLA. Nevertheless, ester linkages do not start hydrolyzing until they are exposed to water and meet certain conditions of pH and temperature. There are no microbes engaged in the initial step of breakdown, which consists only of hydrolysis. Bacteria don't start breaking down lactic acid oligomers with lower molecular weights into carbon dioxide and water until the average molecular weight drops below about 10,000.

In contrast to other biodegradable polymers, PLA undergoes a multi-stage degradation process rather than the one-step process often seen with bacteria attacking the polymeric device directly. When compared to other biodegradable polymers, PLA stands out due to its unique two-stage degrading process. This feature is particularly useful for items' preservation and for applications that include food. Composting speeds up the degradation of PLA under humid, warm conditions (55 to 70 degrees Celsius). Pla goods, on the other hand, have a very high storage stability at lower humidity and temperatures.



Lactic acid or 2-hydroxypropanoic acid (lactic acid 1.2) is the fundamental component of poly (lactic acid). There is a chiral carbon atom in this poly (lactic acid) chain that connects the carboxylic acid and hydroxyl groups. Diastereoisomeric polymer chains of PLA are possible due to this chiral carbon; these chains can be isotactic, syndiotactic, hetero-, or atactic, according to the orientation of the methyl group relative to the chain's propagation direction. Some PLA polymers are semicrystalline, with melting points between 130 and 180 degrees Celsius, whereas others are amorphous glassy, with glass transition temperatures of about 50 to 60 degrees Celsius.

Poly (lactic acid) was first introduced by Carothers in 1932, despite its low molecular weight and inadequate mechanical properties. Some of the most prominent companies in the global chemical industry are now involved in the production of lactic acid and PLA polymers due to the substantial advancements achieved in lactic acid manufacturing through research and development in the years that followed. The most significant companies involved in the lactic acid industry are listed in Table 1.1.

#### SOURCE OF MONOMER:

Both L-lactic acid, whose molecular formula is C<sub>3</sub>H<sub>6</sub>O<sub>3</sub>, and L-lactide, the monomer for poly (lactide), are present in nearly all forms of complex life. Perhaps its most crucial function in animals and humans is its association with the supply of energy to muscle tissues. This aliphatic acid is available in two enantiomeric forms, and it is also very hygroscopic and water-soluble. Dextrorotatory L (+) lactic acid is the most common kind found in nature, while D (-) lactic acid is quite uncommon. There are two separate ways that lactic acid may be mass-produced for industrial usage. A petrochemical (Scheme 1.1) source is one of them; it's a chemical process that produces lactic acid in a 50/50 or racemic form by hydrolyzing acetonitrile.

Table 1. 1 Lactic acid production: Global Scenario

Company	Plant location	Production capacity (in tons)
Purac	Holland, Spain, Brazil	80,000
Purac / Cargill	USA	34,000
Galactic	Belgium	15,000
ADM	USA	10,000
Mitsubishi	Japan	8,000

Another source of lactic acid is the fermentation broth of sugar and starch made by various lactic acid bacteria (LAB).

In this case, the dextrorotatory (D or L (+)) form is almost always present. Worldwide, lactic acid production amounts to 100,000 metric tons per year; around 90% of this comes from fermentation of lactic acid bacteria, with the other 90% being synthetic. Musahino, based in Japan, is the sole manufacturer of the synthetic variety now.

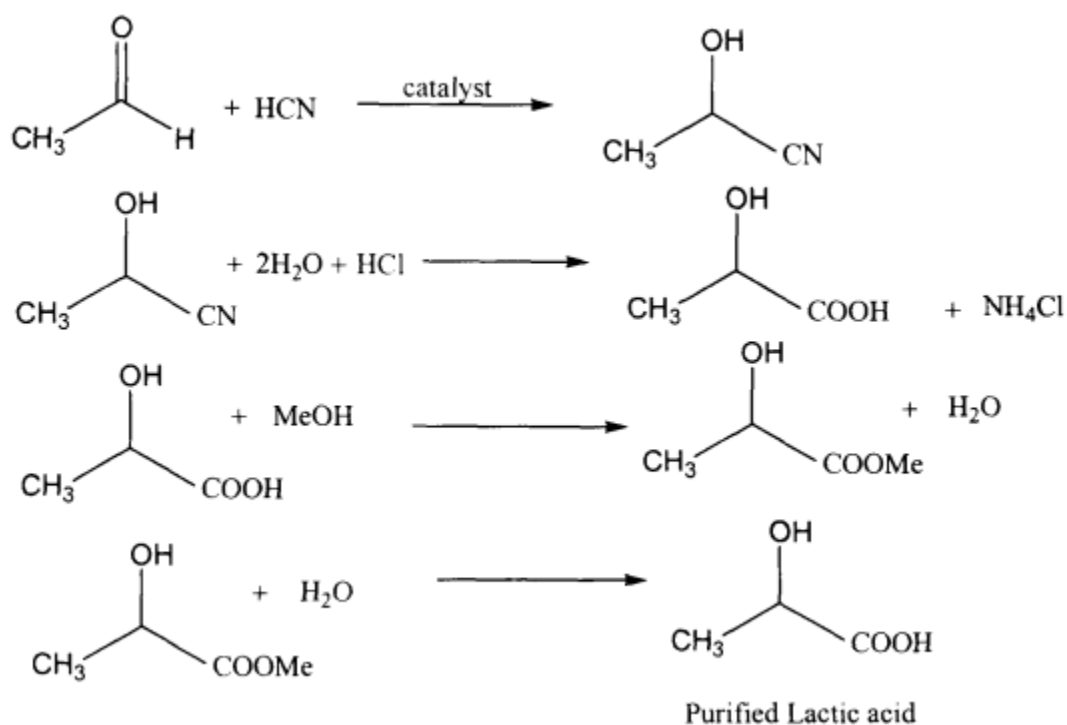
Choosing a strain of lactic acid bacteria (LAB) that generates just one isomer allows one to create an optically pure product when employing fermentation as a source. This is a benefit that the fermenting source offers. The ability to synthesize an enantiomerically pure lactic acid has important consequences for the last structure-property relationship of the PLA. Also, you may find starch, hemicellulose, and cellulose in nature. Lactic acid is produced when these chemicals are digested to mainly glucose and then fermented by a variety of bacteria. Furthermore, there is zero net carbon dioxide emission from these resources to the atmosphere. They can't do photosynthesis and development on their own without consuming carbon dioxide, which is why this is the case.

#### PRODUCTION OF L-LACTIC ACID

It is more significant from an industrial and commercial point of view, in addition to being crucial from an environmental point of view, because the product of lactic acid that is obtained from natural resources that are renewable is more important.

Fermentation route to lactic acid

The creation of lactic acid is the responsibility of a specific type of bacteria known as lactic acid bacteria (LAB), which are responsible for the metabolic cycle by which they function. The following genera are included in the category of lactic acid bacteria (LAB): Carno bacterium, Enterococcus, Lactobacillus, Lactococcus, Leuconostoc, Oenococcus, Pediococcus, Streptococcus, Tetragenococcus, Vagococcus, and Weissella.



**Scheme 1: The synthetic route to lactic acid monomer through acetaldehyde**

Lactic acid is the principal end product that is produced by LAB as a result of the anabolic fermentation of carbohydrates, which is a process that conserves energy. ATP, which stands for adenosine triphosphate, cannot be produced by LAB. The great majority of them are facultative anaerobes and have a high tolerance for acidity, particularly at pH levels that are lower than 5. Temperatures ranging from 20 to 45 degrees Celsius are considered to be optimal for their growth; however, this threshold varies depending on the species. One hundred percent of them are GRAS, which is an abbreviation that stands for "generally regarded as safe." On the other hand, there are strains of bacteria that are thought to be dangerous, such as streptococci. Due to the fact that they do not create vitamins B

and amino acids, they are able to flourish in an environment that has a diverse nutritional profile and digest a broad variety of carbohydrates. However, they are unable to manufacture vitamins B. Each and every LAB have this additional quality, which is of significant value and is shared by all of them.

The most significant microbiological sources of lactic acid are lactic acid bacteria (LAB) and some filamentous fungi that have structures that are filamentous. According to the kind of fermentation that takes place, LAB may be classified into two distinct categories: (1) homofermentative and (2) heterofermentative. Both of these classifications are dictated by one another. When homofermentative LAB is performed, virtually just one product is produced, and that is lactic acid. On the other hand, heterofermentative LAB is capable of producing a wide range of other products in addition to lactic acid. These compounds include ethanol, diacetyl for mate, acetoin or acetic acid, and carbon dioxide.

### Review Of Literature

**Vishakha Chauhan (2022)** Biodegradable polymers could be degraded by bacteria and other microorganisms in due time. In order for the body to metabolize or eliminate tiny, harmless molecules, enzymes hydrolyze and oxidize biodegradable polymers. Very little damage is done to the environment by biodegradable polymers and their byproducts. People sometimes refer to biodegradable polymers as "smart polymers" because of their remarkable capacity to adapt to subtle alterations in their surrounding environment. The use of smart biodegradable polymers to release encapsulated pharmaceuticals at specified areas and times in response to physiological cues is a promising strategy for medication administration. Environmental variables such as light, temperature, pH, and chemical concentrations can have a profound effect on smart polymeric materials.

**Seyma Karaismailoglu (2018)** This research takes a close look at a number of different approaches to making and researching polymeric nanoparticles. Nanoparticles are solid or colloidal particles of macromolecular substances that are less than 100 nanometers in size. Numerous biological fields rely heavily on nanoparticles, including molecular imaging, biosensing, biological separation, and anticancer medicines. Nanoscale materials and the novel features and functionalities they provide are radically distinct from their bulk counterparts. Numerous novel properties are exhibited by these materials as a result of their enhanced resolution, high volume/surface ratio, and multifunctional capacities.

**Geszke-Moritz (2024)** An emphasis shifted to studies examining the biodegradable polymeric nanoparticle systems employed by modern drug delivery systems. Several polymers, such as PLGA, PLA, PEG-based copolymers, and polymers that were spontaneously generated, were thoroughly examined in this study. Their vital role in improving site-specific targeting through surface modification approaches, controlling and prolonging release, preventing early degradation of sensitive medicinal chemicals, and boosting drug solubility was shown.

**Idrees et al. (2020)** Chitosan, alginate, gelatin, and dextran are examples of natural biodegradable polymers that were the subject of extensive research into nanoparticle fabrication. The writers covered a lot of ground, including the physicochemical properties, encapsulating tactics, and several production methods for these polymers. Their research shown that natural polymers have several benefits, including improved biocompatibility, reduced immunogenicity, and ecologically benign disintegration, that make them ideal for targeted medication delivery and biological applications.

**Mathane et al. (2025)** Within the context of the evaluation of polymers that are employed in nanoparticle-based drug delivery systems, a significant amount of emphasis was placed on the qualities that were utilized to choose the biodegradable polymer. According to the authors, the loading capacity of the drug, the release kinetics, and the efficiency of the targeting are all impacted by characteristics such as hydrophilicity, mechanical strength, rate of degradation, and crystallinity. In addition, the study highlighted the most recent developments in polymer blends, copolymers, and hybrid systems, all of which were designed to improve the effectiveness of pharmaceutical products while simultaneously minimizing adverse effects.

**Rho (2025)** polymeric nanoparticles that were used for drug delivery experiments were investigated, along with the fundamental functional characterization procedures required for them. Throughout the course of the research, a wide range of analytical methods were given considerable attention. Structural morphology was assessed by electron microscopy, surface charge was determined by zeta potential, and in vitro drug release was determined by various techniques. Size was determined by dynamic light scattering. According to the author, precise physicochemical characterization is essential for establishing a connection between the features of nanoparticles and their biological

performance, biodistribution, and therapeutic results.

**Dixit (2025)** The topic of discussion was targeted drug carriers that were constructed of polymeric nanoparticles, with an emphasis on active targeting approaches like as receptor-mediated delivery, antibody attachment, and ligand conjugation. In the review, the potential advantages of surface functionalization were emphasized. These advantages include the enhancement of cellular uptake, therapeutic specificity, and treatment effectiveness with minimal off-target harm. Because of the significant therapeutic potential of targeted polymeric nanoparticles in the treatment of cancer and inflammatory illnesses, these conditions were the key areas of focus for researchers.

### MATERIALS AND EQUIPMENTS

#### CHEMICALS USED IN THE STUDY

*Table 1 A list of the substances and compounds that were utilized in the research*

Serial No	Name	Source
1.	Acetone	Merck Life Science Pvt. Ltd, Bengaluru, India
2.	Acetonitrile	Merck Life Science Pvt. Ltd, Bengaluru, India
3.	Cell lysis buffer	Abcam
4.	Cetuximab	Ideal Chemicals, Kolkata, India
5.	Chloroform	Merck Life Science Pvt. Ltd, Bengaluru, India
6.	Citric acid	Merck Life Science Pvt. Ltd, Bengaluru, India
7.	4',6' Diamidino-2-phenylindole (DAPI)	Thermo Fisher Scientific, Mumbai, India
8.	Dichloromethane (DCM)	Merck Life Science Pvt. Ltd, Bengaluru, India
9.	Disodium hydrogen phosphate	Merck Life Science Pvt. Ltd, Bengaluru, India
10.	Dimethyl sulfoxide (DMSO)	Merck Life Science Pvt. Ltd, Bengaluru, India
11.	Dulbecco's Modified Eagle Medium (DMEM)	Thermo Fisher Scientific, Waltham, USA
12.	Ethylene diamene tetra acetic acid (EDTA)	Merck Life Science Pvt. Ltd, Bengaluru, India

13.	1-(3-dimethylaminopropyl)-ethylcarbodiimide hydrochloride (EDC)	3-	HiMedia Laboratories Pvt. Ltd., Maharashtra, Mumbai, India.
14.	Ethyl Acetate		Merck Life Science Pvt. Ltd, Bengaluru, India India
15.	Fetal bovine serum (FBS)		HiMedia Laboratories, Mumbai, India
Serial No	Name		Source
16.	Fluorescein isothiocyanate (FITC)		HiMedia Laboratories, Mumbai, India
17.	FITC annexin V/dead cell apoptosis kit		Thermo Fisher Scientific, Waltham, MA, USA
18.	Glacial acetic acid		Merck Life Science Pvt. Ltd, Bengaluru, India
19.	Methanol		Merck Life Science Pvt. Ltd, Bengaluru, India
20.	3-(4,5-dimethylthiazol-2-yl)-diphenyltetrazolium bromide (MTT)	2,5-	HiMedia Laboratories, Mumbai, India
21.	N-hydroxy succinimide (NHS)		HiMedia Laboratories Pvt. Ltd., Maharashtra, Mumbai, India.
22.	Docetaxel (DTX)		A gift samples provided by Fresenius Kabi Oncology, Kolkata, West Bengal, India with 99.95% purity
23.	Penicillin-Streptomycin		HiMedia Laboratories, Mumbai, India
24.	Acid-terminated Poly lactic-co-glycolic acid (ratio, 75:25; molecular weight, 4,000–15,000 Da)		Sigma-Aldrich Co, St Louis, MO, USA.
25.	Potassium dihydrogen phosphate		Merck Life Science Pvt. Ltd, Bengaluru, India
26.	Polyvinyl alcohol (M.W. 85,000-1,24,000) (M.W. 150,000)		SD Fine-Chemicals limited, Mumbai, India

27.	Roswell Park Memorial Institute Medium (RPMI 1640)	HiMedia Laboratories, Mumbai, India
28.	Sodium acetate	Merck Life Science Pvt. Ltd, Bengaluru, India
29.	Sodium bicarbonate	Merck Life Science Pvt. Ltd, Bengaluru, India
Serial No	Name	Source
30.	Sodium carbonate	Merck Life Science Pvt. Ltd, Bengaluru, India
31.	Sodium citrate	Merck Life Science Pvt. Ltd, Bengaluru, India
32.	Sodium hydroxide	Merck Life Science Pvt. Ltd, Bengaluru, India
33.	Trypsin	HiMedia Laboratories, Mumbai, India
34.	Tween 80	SD Fine Chemicals limited, Mumbai, India
35.	Water for HPLC Corp. Billerica, MA, USA 41. Millex-GP Syringe Filter Unit, 0.22 $\mu$ m, polyethersulfone, 33 mm, gamma sterilized Millipore Corp. Billerica, MA, USA	Merck Life Sc. Pvt. Ltd., Mumbai, Maharashtra, India
36.	Milli-Q water Millipore	Corp. Billerica, MA, USA

### Methodology

#### Docetaxel absorbance maximum ( $\lambda_{max}$ ) estimation using UV-visible spectroscopy

A combination of acetonitrile and water in a 60:40 v/v ratio was used to create a solution of docetaxel (10  $\mu$ g/ml). Scan the solution with an absorption spectrophotometer from 200 nm to 400 nm, using an acetonitrile:water combination as a blank, to find the drug's absorbance maxima ( $\lambda_{max}$ ).

#### Preparation of stock solution of drug

To make the main stock solution of docetaxel, 1 milligram of the drug was dissolved in 10 milliliters of a 60:40 v/v combination of acetonitrile and water. A strong regression coefficient ( $R^2=0.999$ ) was obtained, which was in accordance with Beer's law and indicated a linear relationship between drug concentration and absorbance.

#### Preparation of calibration curve of drug solution

In a mixture of acetonitrile and water, various portions ranging from half a milligram to ten micrograms per milliliter were generated from the docetaxel stock solution (1 mg/10 ml). The absorption peaks ( $\lambda_{max}$ ) were then measured at 229 nm using a UV-Visible spectrophotometer, with acetonitrile: water used as a control. The data is shown as the mean  $\pm$  standard deviation, and it was measured three times. By plotting the absorbance versus the concentrations, we were able to get the slope and regression coefficient ( $R^2$ ).

## RESULTS

### Determination of absorbance maxima ( $\lambda_{max}$ ) of Docetaxel

The analytical wavelength of 229 nm in the acetonitrile:water solution was chosen due to the fact that, while scanning Docetaxel using a spectrophotometric technique, the maximum wavelength ( $\lambda_{max}$ ) was reached at that concentration. Figure 1 displayed the docetaxel absorbance spectrum.

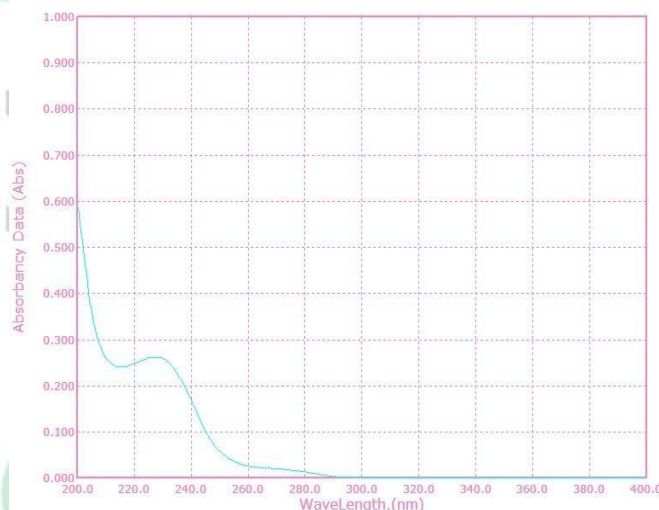


Figure 1 Absorbance maxima ( $\lambda_{max}$ ) of Docetaxel

### Estimation of calibration curve of Docetaxel

Throughout the concentration range of 0.5 to 10  $\mu\text{g/ml}$ , the drug's absorbance values were measured at 229 nm when dissolved in acetonitrile: water. A strong regression coefficient ( $R^2=0.999$ ) was obtained, which was in accordance with Beer's law and indicated a linear relationship between drug concentration and absorbance. Figure 2 shows the Docetaxel calibration curve in an acetonitrile:water solution.

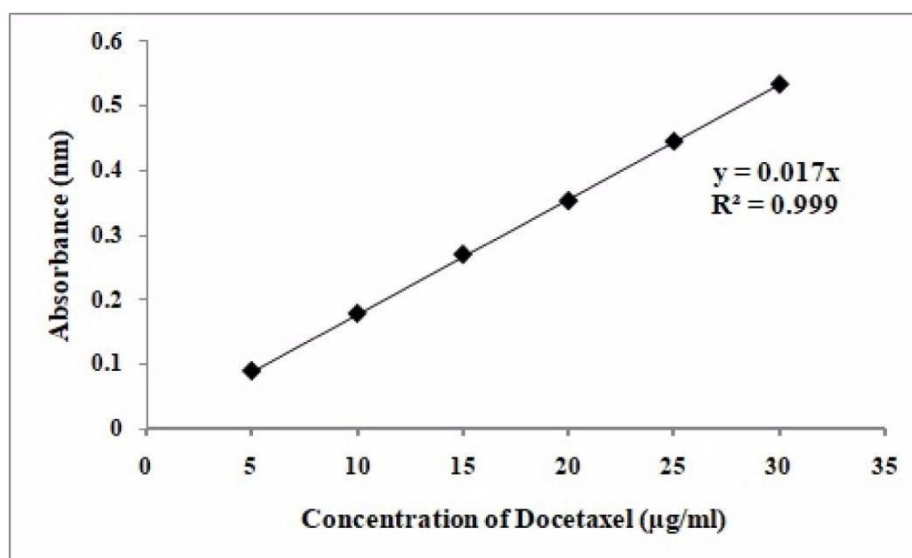


Figure 2 Calibration curve of Docetaxel in acetonitrile: water

### Fourier Transform Infrared Spectroscopy (FTIR) analysis

The spectrophotometric analysis picked up on all the DTX and excipient peaks that went into making DTX NP. According to Figure 3, there were no signs of any chemical interactions between the two. The presence of N-H

stretching at 3490  $\text{cm}^{-1}$  and symmetric and asymmetric vibrations at 2947  $\text{cm}^{-1}$  for  $\text{CH}_2$  were detected in pure DTX. Peaks at 1725  $\text{cm}^{-1}$  and 1244  $\text{cm}^{-1}$  for  $\text{C}=\text{O}$  stretching vibrations and 1075  $\text{cm}^{-1}$  for  $\text{C}=\text{N}$  stretching vibrations were seen in the ester group, respectively. The maxima were seen at 972  $\text{cm}^{-1}$  for  $\text{C}-\text{H}$  in-plane and 712  $\text{cm}^{-1}$  for  $\text{C}-\text{H}$  out-of-plane  $\text{C}-\text{C}=\text{O}$ .  $\text{O}-\text{H}$  at 3515  $\text{cm}^{-1}$ ,  $\text{C}-\text{H}$  at 2995  $\text{cm}^{-1}$ , and  $\text{C}=\text{O}$  at 1756  $\text{cm}^{-1}$  were the distinctive peaks that PLGA exhibited.

Blank NP and DTX NP showed some small peak shiftings of the formulation components due to weak physicochemical interactions, such as dipole-induced interaction, weak H-bonds, van der Waals force of attraction, etc., which could play a big role in the formation of spherical nanoparticles. The strength of the 712  $\text{cm}^{-1}$  peak in the spectra of the physical combination (PLGA, PVA and DTX) and DTX NP indicates that DTX is trapped over the blank NP.

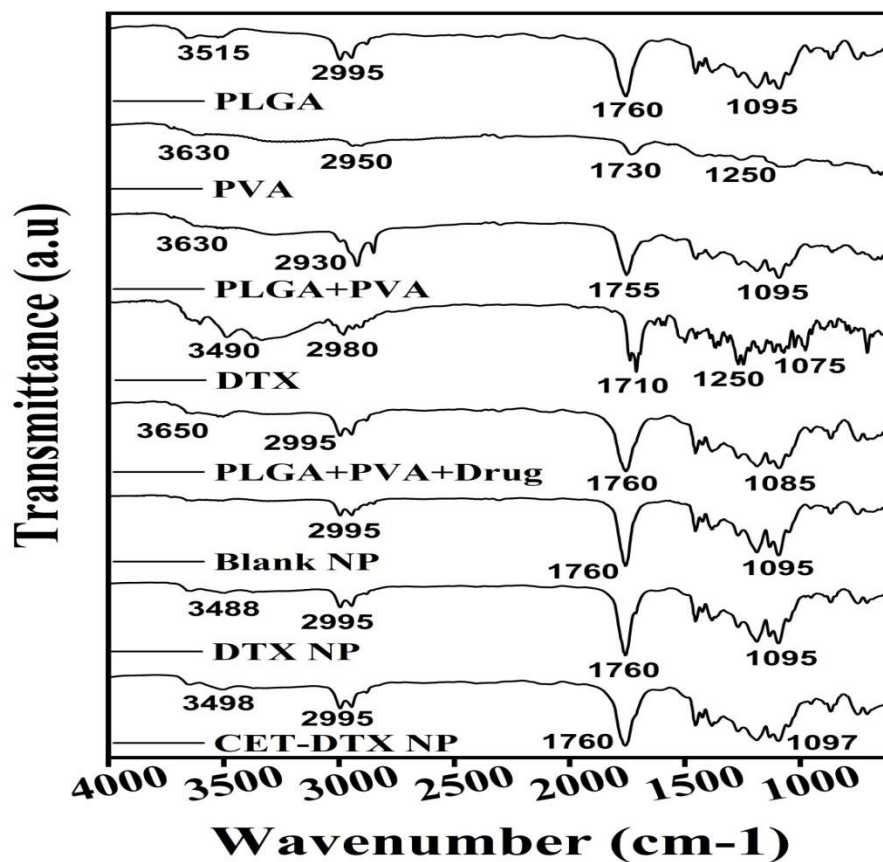


Figure 3 Poly lactic-co-glycolic acid (PLGA)

Nanoparticulate formulations, physical mixtures, and individual component FTIR spectra are shown in Figure 3. Poly lactic-co-glycolic acid (PLGA), polyvinyl alcohol (PVA), docetaxel (DTX), blank nanoparticles (NP), docetaxel-loaded nanoparticles (NP), and cetuximab conjugated nanoparticles (CET-DTX NP) are all part of the same physical composition.

Table 2 shows the results of an experiment that varied the drug polymer ratio of different nanoparticles in order to determine their drug loading and encapsulation effectiveness. According to the results, the best DTX NP had the highest drug loading and entrapment efficiency. The drug loading efficiency for DTX NP was measured at  $6.43\% \pm 0.25\%$ , whereas the encapsulation efficiency was  $70.76\% \pm 2.76\%$ . The drug loading efficiency for Cet-DTX NP was determined to be  $5.86 \pm 0.35\%$  and the encapsulation efficiency to be  $64.53\% \pm 1.38\%$ .

Table 2 Optimizing The Physicochemical Properties Of Different Experimental Nanoparticles By Manipulating The Drug: Polymer Ratio

Formulation	Drug:PLGA	Particle size (Z-average) (nm) <sup>a</sup>	Zeta potential (mV) <sup>a</sup>	Polydispersity index <sup>a</sup>	Drug loading (%) <sup>a</sup>	Encapsulation efficiency (%) <sup>a</sup>
DTX NP (optimized formulation)	1:10	225 ± 3	-8.18 ± 0.50	0.589 ± 0.060	6.43% ± 0.25%	70.76% ± 2.76%
Cet-DTX NP (optimized formulation with antibody conjugation)	1:10	283 ± 2	-12.10 ± 0.43	0.486 ± 0.080	5.86% ± 0.35%	64.53% ± 1.38%
DTX NP 1	2:10	400 ± 2	-5.10 ± 0.47	0.663 ± 0.060	5.06% ± 0.05%	55.73% ± 0.50%
DTX NP 2	3:10	456 ± 2	-4.40 ± 0.29	0.609 ± 0.040	4.72% ± 0.07%	51.92% ± 0.78%

The abbreviations DTX NP and Cet-DTX NP stand for "poly (lactide-co-glycolide) nanoparticles encapsulating docetaxel," "PLGA" for "poly vinyl alcohol," and "n = 3" for each of the other terms.

#### Particle size and zeta potential

Table 1 provides information on the values of the polydispersity index (PDI), as well as the particle size and zeta potential of the produced nanoparticles. In order to properly characterize the physicochemical properties of the improved formulation of DTX NP and Cet-DTX NP, testing was performed. Both DTX NP and Cet-DTX NPs were found to have particle sizes of  $225 \pm 3$  nm and  $283 \pm 2$  nm, respectively, according to the findings of the study. Figure 6.4 illustrates that the zeta potential value of DTX nanoparticles (NP) and Cet-DTX nanoparticles (NPs) was  $-8.18 \pm 0.50$  mV and  $-12.1 \pm 0.43$  mV, respectively. There was a significant difference in the PDI value between DTX NP, which was  $0.589 \pm 0.060$ , and Cet-DTX NP, which was  $0.486 \pm 0.080$ .

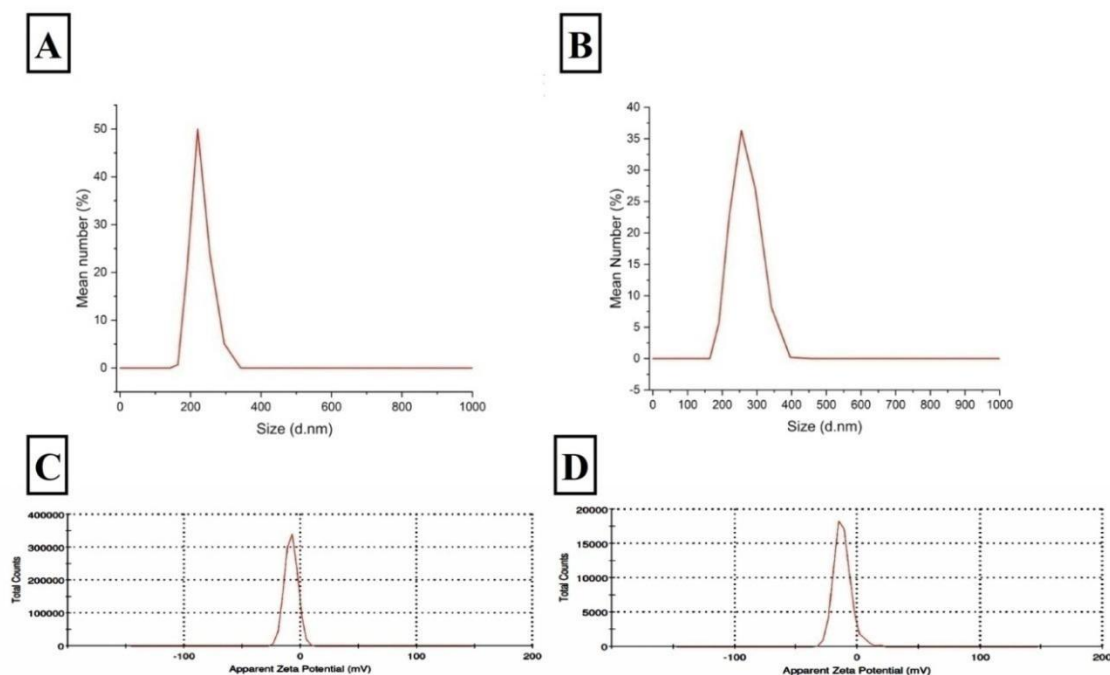


Figure 4 Particle size of DTX nanoparticles

The results for the zeta potential and the particle size distribution are shown in Figure 4. Particle size of DTX nanoparticles (A) and (B) The Zeta potential data of DTX NP, the particle size of Cet-DTX NP, and the Zeta potential data of Cet-DTX NP are presented in the following order: (C)

#### Surface morphology of the nanoparticles

Studies using field emission scanning electron microscopy (FESEM) were conducted in order to investigate the surface morphology of Cet-DTX nanoparticles (Figure 5.A). It was clear from the figure that the bulk of the Cet-DTX nanoparticles had a spherical form and were densely dispersed. The interior morphology of Cet-DTX NP was validated by the utilization of transmission electron microscopy (Figure 4.5B). As a result of the figures, it was discovered that the medicine was spread uniformly and uniformly across the particles.

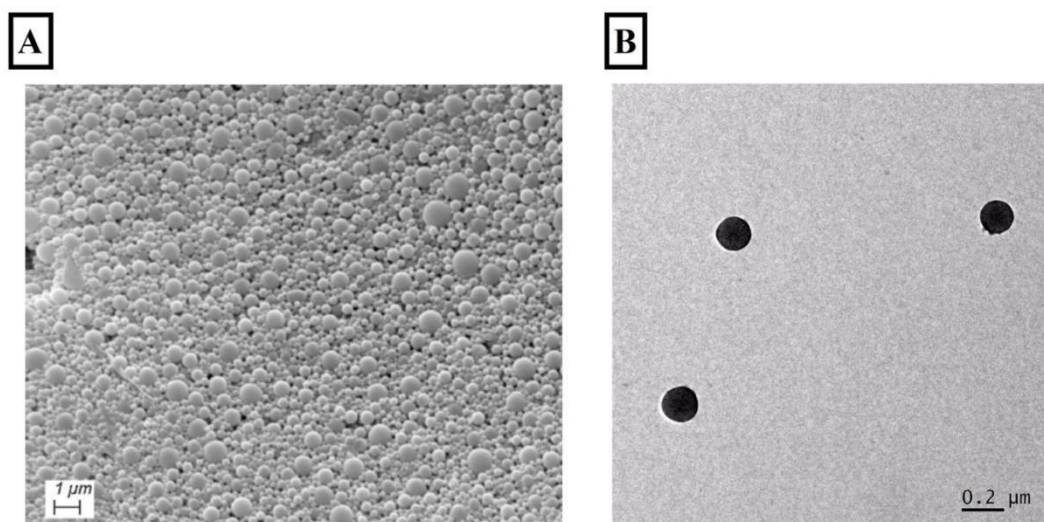


Figure 5 Energy dispersive X-ray (EDX) analysis

Figure 5. (A) At a magnification of 10,000 times, field emission scanning electron microscopy was performed on Cet-DTX nanoparticles. (B) Transmission electron microscopy was performed on Cet-DTX nanoparticles. Energy dispersive X-ray (EDX) analysis was performed. Additionally, the EDX research for blank NP, DTX NP, and Cet-DTX NP was carried out in conjunction with the FESEM analysis. The presence of nitrogen in the case of DTX nanoparticles (NP) and the absence of nitrogen in the case of blank nanoparticles (NP) showed the presence or absence of nitrogen in DTX in the relevant formulations.

#### DISCUSSION

Despite being one of the most frequently discovered tumors worldwide, treating non-small cell lung cancer (NSCLC) remains challenging. According to reports, a large number of human cancers exhibit abnormal signaling and most non-small cell lung cancer (NSCLC) instances include overexpression of the epidermal growth factor receptor (EGFR). It has been linked to increased tumor proliferation, poor tumor differentiation, and greater risks of lymph node metastases (Hsu et al., 2019). A poorer prognosis has also been linked to it. The ability to precisely target medications to tumor sites using tumorspecific ligands, such as antibodies on nanoparticle surfaces against specific receptors, is well-known (Tian et al., 2022). Through the development of antibody linked nanoparticles loaded with covalently bound Cet antibody against EGFR, we were able to target malignant lung cells and create a nanoformulation that could deliver the medicine to the affected cells.

Because of its remarkable anti-proliferative qualities, DTX was added to the PLGA nanoparticles to enhance the drug's potential for cancer treatment. A research using Fourier transform infrared spectroscopy (FTIR) was conducted on DTX NP, which showed a little shifting of the drug's non-typical peaks. Physical interactions through bond forms, including electrical forces like dipole moments and van der Waals forces and weak hydrogen bond formation, could account for this discovery. The presence of all the expected DTX peaks in DTX NP, however, indicates that the drug's molecular structure is preserved within the nanoparticles. The Cet antibody was effectively coupled with the surface of the PLGA NP using the EDC/NHS coupling chemistry (Mondal et al., 2019). By manipulating the ratio of

medication to polymer, the nanoformulations were created. Particle size was affected by the enhancement of drug content. The cohesion of the polymeric molecules was diminished due to drug entrapment towards the core and inside and between the chains, leading to a rise in particle size. The results show that surface conjugation of cetuximab (Cet) clearly increases particle size (Table 6.1). Since the produced nanoparticles will interact with biological membranes prior to absorption, their surface shape is crucial. In addition to a uniform drug distribution and a smooth, spherical surface, the nanoformulations were also devoid of aggregation. The negative zeta potential of Cet-DTX NPs, which is generated by the presence of a -COOH group in the polymer, falls within the range of -30 to +30 mV. As a result, these nanoparticles must be kept as lyophilized powder and reconstituted in dispersed form before to use (Dutta et al., 2019).

## CONCLUSION

Our current study aims to address the overexpression of EGFR receptors in malignant lung cells (A549 and NCI-H23) by developing a targeted nanoformulation (CetDTX NP) that can deliver the anticancer medication DTX to these cells. To integrate a larger concentration of medication, the PLGA nanoparticles were created using the multiple emulsion solvent evaporation process. In addition, the carboxyl terminal group of PLGA that is exposed to the nanoparticles' surface allows for further surface functionalization of the antibody. The results of this study proved that biodegradable PLGA nanoparticles endowed with Cet and the necessary physicochemical qualities were effectively loaded with the powerful anti-cancer medication DTX. Cet binding to the drug-loaded nanoparticles also allowed for site-specific targeting of DTX to lung cancer cells that overexpress EGFR receptors, resulting in a gradual and prolonged release of the medication. In terms of therapeutic improvement, the Cet-DTX NP outperformed both free DTX and DTX NP, according to the results of *in vitro* and *in vivo* tests. Cet-DTX NP had the greatest capacity for cellular uptake and cell death, primarily because it bound to lung cancer cells with such a strong affinity. When administered to mice with lung cancer that had been generated by B(a)P, Cet-DTX NP dramatically decreased the number of malignant lung lesions.

## REFERENCES

- [1] Abou-El-Naga AM, Mutawa G, El-Sherbiny IM, Mousa SA. Activation of Polymeric Nanoparticle Intracellular Targeting Overcomes Chemodrug Resistance in Human Primary Patient Breast Cancer Cells [Retraction]. *Int. J. Nanomedicine* 2022;17:25552556.
- [2] Aggarwal S, Gupta S, Pabla D, Murthy RS. Gemcitabine-loaded PLGA-PEG immunonanoparticles for targeted chemotherapy of pancreatic cancer. *Cancer Nanotechnol.* 2013;4:145-157.
- [3] Ahmed MM, Fatima F, Anwer MK, Aldawsari MF, Alsaidan YS, Alfaiz SA, Haque A, Alanazi AZ, Alhazzani K. Development and characterization of Brigatinib loaded solid lipid nanoparticles: In-vitro cytotoxicity against human carcinoma A549 lung cell lines. *Chem. Phys. Lipids* 2020;233:105003.
- [4] Alexis F, Rhee JW, Richie JP, Radovic-Moreno AF, Langer R, Farokhzad OC. New frontiers in nanotechnology for cancer treatment. In: *Urologic Oncology: Seminars and Original Investigations* 2008 (Vol. 26, No. 1, pp. 74-85). Elsevier.
- [5] Alfieri RR, Galetti M, Tramonti S, Andreoli R, Mozzoni P, Cavazzoni A, Bonelli M, Fumarola C, La Monica S, Galvani E, De Palma G. Metabolism of the EGFR tyrosin kinase inhibitor gefitinib by cytochrome P450 1A1 enzyme in EGFR-wild type non small cell lung cancer cell lines. *Mol. Cancer* 2011;10:1-14.
- [6] Aran V, Omerovic J. Current approaches in NSCLC targeting K-RAS and EGFR. *Int. J. Mol. Sci.* 2019;20:5701.
- [7] Assoun S, Brosseau S, Steinmetz C, Gounant V, Zalzman G. Bevacizumab in advanced lung cancer: state of the art. *Future Oncol.* 2017;13:2515-2535.
- [8] Attia MF, Anton N, Wallyn J, Omran Z, Vandamme TF. An overview of active and passive targeting strategies to improve the nanocarriers efficiency to tumour sites. *J. Pharm. Pharmacol.* 2019;71:1185-1198.
- [9] Azimi B, Nourpanah P, Rabiee M, Arbab S. Poly (lactide -co- glycolide) Fiber: An Overview. *J. Eng. Fiber. Fabr.* 2014; 9:47-66.
- [10] Bagnardi V, Rota M, Botteri E, Scotti L, Jenab M, Bellocco R, Tramacere I, Pelucchi C, Negri E, La Vecchia C, Corrao G. Alcohol consumption and lung cancer risk in never smokers: a meta-analysis. *Ann. Oncol.* 2011;22:2631-2639.

- [11] Baker S, Dahele M, Lagerwaard FJ, Senan S. A critical review of recent developments in radiotherapy for non-small cell lung cancer. *Radiat. Oncol.* 2016;11:1-14.
- [12] Barak D, Engelberg S, Assaraf YG, Livney YD. Selective Targeting and Eradication of Various Human Non-Small Cell Lung Cancer Cell Lines Using Self-Assembled Aptamer-Decorated Nanoparticles. *Pharmaceutics* 2022;14:1650.
- [13] BarathManiKanth S, Kalishwaralal K, Sriram M, Pandian SR, Youn HS, Eom S, Gurunathan S. Anti-oxidant effect of gold nanoparticles restrains hyperglycemic conditions in diabetic mice. *J. Nanobiotechnology* 2010;8:1-15.
- [14] Barua A, Choudhury P, Nag N, Nath A, Kundagrami S, Pal A, Panda CK, Saha P. Xanthone from *Swertia chirata* exerts chemotherapeutic potential against colon carcinoma. *Curr. Sci.* 2022;122:47-55.

IJEETE

